CHEMISTRY
A European Journal

Supporting Information

How Outer Coordination Sphere Modifications Can Impact Metal Structures in Proteins: A Crystallographic Evaluation

Leela Ruckthong,[a, b] Jeanne A. Stuckey,[c, d] and Vincent L. Pecoraro*[a]

chem_201806040_sm_miscellaneous_information.pdf

Author Contributions

V.P. Conceptualization: Lead; Funding acquisition: Lead; Investigation: Lead; Project administration: Lead; Resources: Lead; Supervision: Lead; Writing - Review & Editing: Lead
L.R. Data curation: Lead; Formal analysis: Lead; Investigation: Lead; Methodology: Lead; Validation: Lead; Visualization: Lead; Writing - Original Draft: Lead
J.S. Funding acquisition: Supporting; Investigation: Supporting; Project administration: Supporting; Resources: Lead; Software: Lead; Supervision: Supporting; Validation: Supporting; Writing - Review & Editing: Supporting.

SUPPORTING INFORMATION

How Outer Coordination Sphere Modifications Can Impact Metal Structures in Proteins: A Crystallographic Evaluation

Leela Ruckthong[1,2], Jeanne A. Stuckey[3,4], Vincent L. Pecoraro[1]*

[1]Department of Chemistry, University of Michigan, Ann Arbor, Michigan 48109, USA
[2]Department of Chemistry, Faculty of Science, King Mongkut's University of Technology, Thonburi (KMUTT), Bang Mod, Thung Khru, Bangkok, 10140, Thailand
[3]Life Sciences Institute, University of Michigan, Ann Arbor, Michigan 48109, USA
[4]Department of Biological Chemistry, University of Michigan, Ann Arbor, Michigan 48109, USA
*To whom correspondence should be addressed. E-mail: vlpec@umich.edu

Table of Content **page**

Supporting Information Discussion

We were unable to crystallize the CS peptide with two mutations, D-Leu and Cys, due to the instability of peptide folding. It was previously found that the helical property of CS was mildly disrupted with the incorporation of a Cys residue in one of the hydrophobic layers[1–4]; however, in combination with D-Leu, the instability of the CSL12$_D$LL16C grew, subsequently resulting in poor peptide folding **(Supporting information Figure S13)**. The denaturation titration curve of CSL12$_D$LL16C did not follow a two state model changing from the completely folded 3SCC to the unfolded monomer states. This observation demonstrates low propensity for the peptide to fold into a native state. Similarly, the peptide does not show a reasonable percent folding, even in the absence of denaturant where only 30% folding was observed at 10 μM peptide concentration. This value is about 50% less than the percent folding determined for TRIL12$_D$LL16C.[5] Therefore, in order to increase the stability of the construct and enhance folding, the variant was prepared using the elongating GRAND-CS. As predicted, the resulting GRAND-CSL12$_D$LL16C peptide has significantly greater stability. The initial folding of this new design increased to 78± 0.5%. The denaturation titration curve of the apo-peptide shows a significant improved stability with $\Delta G_{folding}$ of 3.02±0.16 kcal/mole[6] and the midpoint (C_m) of 1.85 M of [GuaHCl]. This evidence suggests that the addition of a D-amino acid combined with a Cys residue in GRAND-CSL12$_D$LL16C is well-tolerated. Moreover, when Cd(II) was added to the peptide, ^{113}Cd NMR showed the exact chemical shift as was observed for TRIL12$_D$LL16C (697 ppm) which clearly demonstrates that the metal environment between these two metal binding sites are identical **(Supporting information Figure S14)**. Thus, GRAND-CSL12$_D$LL16C could reasonably serve as a crystallographic analog for TRIL12$_D$LL16C.

Similarly, we have also used the GRAND-CSL16CL19$_D$L analogue to represent the X-ray crystallographic insight for TRIL2WL16CL19$_D$L design. The GRAND-CSL16CL19$_D$L shows less stability compared to GRAND-CSL12$_D$LL16C. The apo-peptide has $\Delta G_{folding}$ of 2.12±0.05 kcal/mole[6] with C_m= 1.46 M and the Cd(II)-peptide of 2.60±0.03 kcal/mole with C_m= 1.83 M. The peptide binds to Cd(II) results in a chemical shift of 600 ppm which is similar to the chemical shift reported for Cd(II)(TRIL2WL16CL19$_D$L)$_3^-$.[6]

Supporting Information Figures

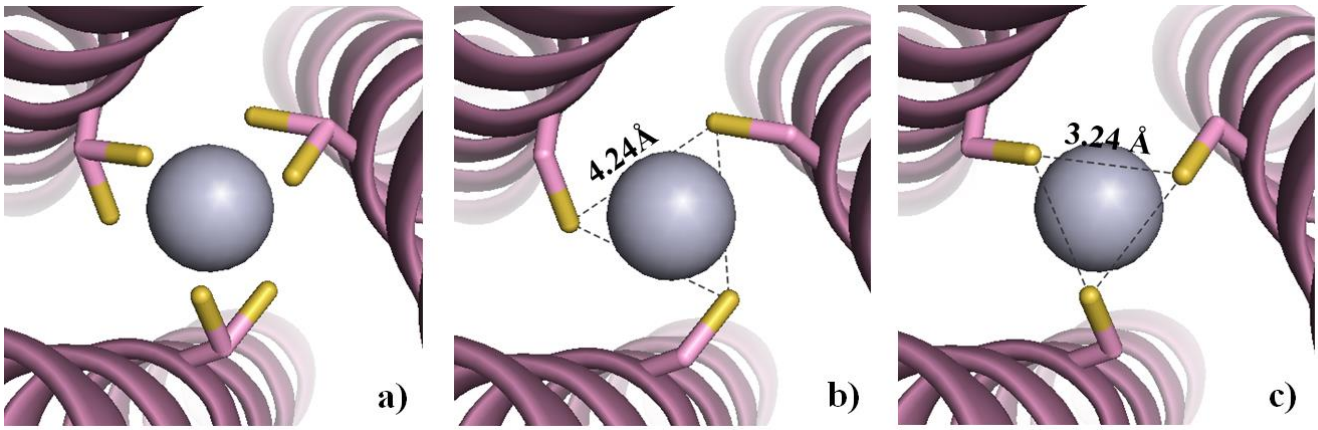

Figure S1. Cys side chain arrangements in the sixteenth position of Hg(II)(GRAND-CSL12AL16C)$_3^-$. The Cys side chains are shown as sticks in which the thiol groups are labelled in yellow. Shown from a top-down view, the structure represents a) both alternate conformers of Cys residues, b) the major conformers and c) the minor (unbound) conformers.

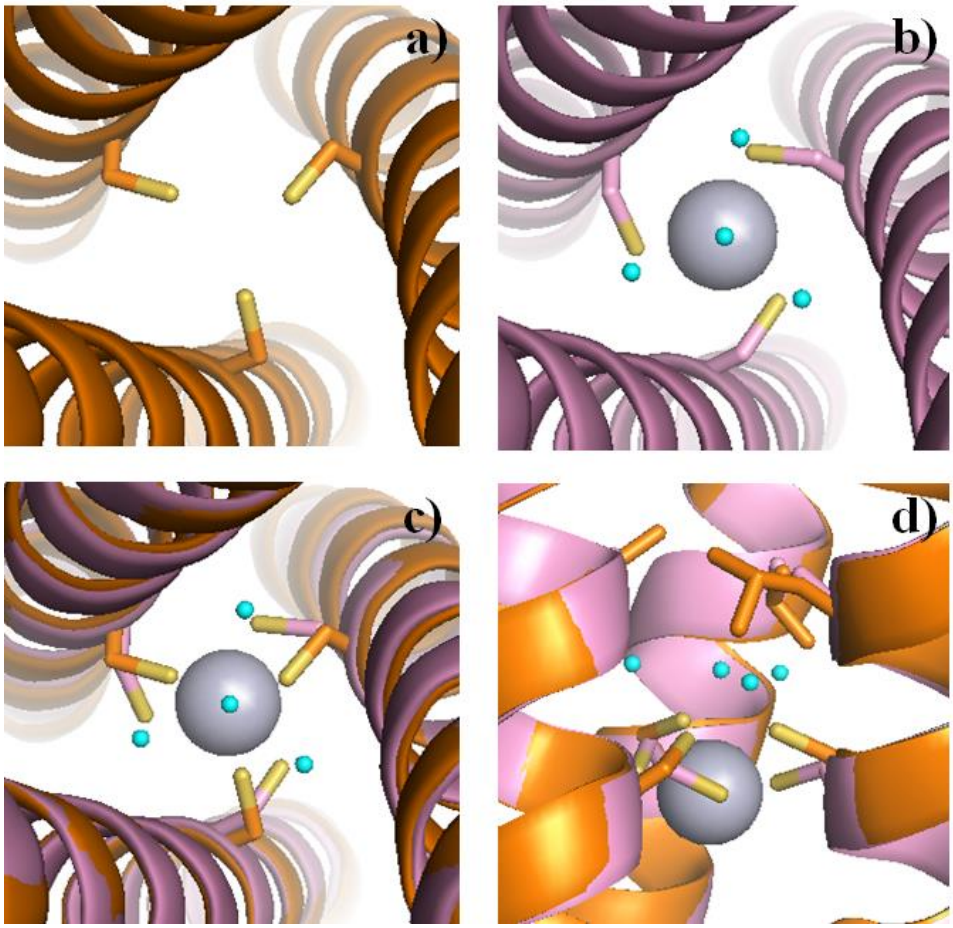

Figure S2. Ribbon diagrams demonstrating an overlay of the cysteine-substituted sixteenth layer between Hg(II)(GRAND-CSL12AL16C)$_3^-$ and apo-(CSL16C)$_3$. Top down (N-termini) view of the major conformer of Cys residues in a) apo-(CSL16C)$_3$ and b) Hg(II)(GRAND-CSL12AL16C)$_3^-$. c) Top down and d) side on views of the overlay showing the predisposition of three Cys ligands toward Hg(II) binding. Main chain atoms of Hg(II)(GRAND-CSL12AL16C)$_3^-$ are pink and apo-(CSL16C)$_3$ are orange. 16Cys (sulfurs=yellow) and 12Ala residues (in d)) are shown as sticks. Hg(II) is present as a gray sphere and the waters observed in between the 12Ala and 16Cys cavity as cyan spheres.

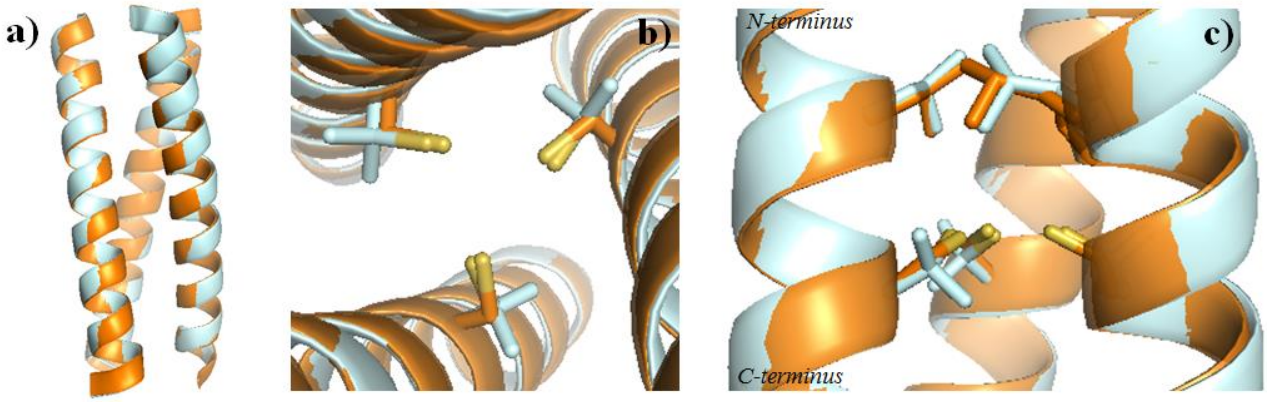

Figure S3. Overlay of the apo-$(CSL16C)_3$ (PDB code: 5K92)[7] with the apo-$(CSL16Pen)_3$ [3]. In a) an excellent alignment of the peptide backbones between apo-$(CSL16C)_3$ and apo-$(CSL16Pen)_3$ indicating that the incorporation of a non-natural amino acid, Pen does not perturb the secondary structure of the 3SCC. In b) comparison of the sixteenth layer between the Cys ligands from apo-$(CSL16C)_3$ and Pen ligands from apo-$(CSL16Pen)_3$ in the top-down and c) side-on views. Main chain atoms of apo-$(CSL16C)_3$ are colored in orange and apo-$(CSL16Pen)_3$ in pale teal. Cys, Pen and Leu (above the metal site) are shown as sticks.

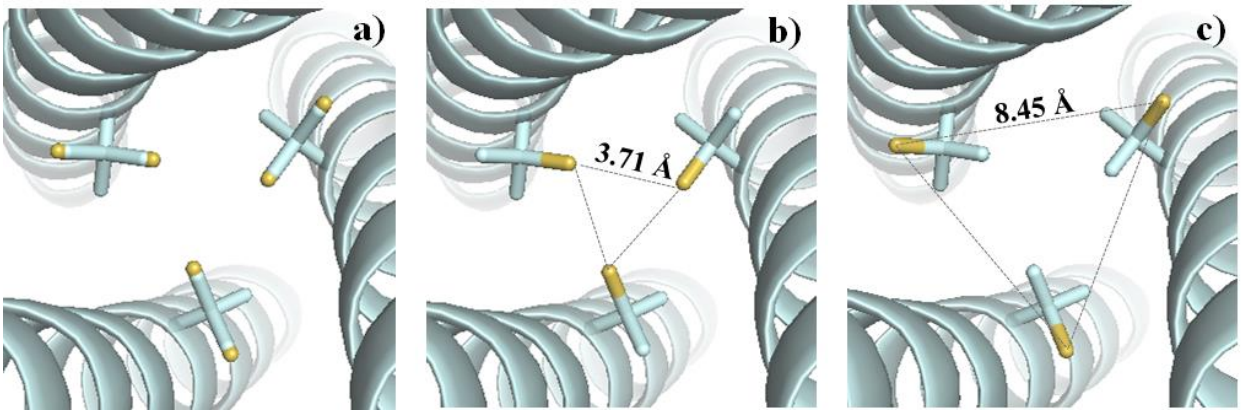

Figure S4. Ribbon diagrams of apo-(CSL16Pen)$_3$ (PDB code: 3H5F)[3] showing the orientation of Pen side chains. Main chain atoms are shown in ribbon diagram and the Pen side chains are in sticks (sulfurs=yellow). Top-down view from N-termini showing the exclusive orientations of a) all conformers, b) major conformers and c) minor conformers.

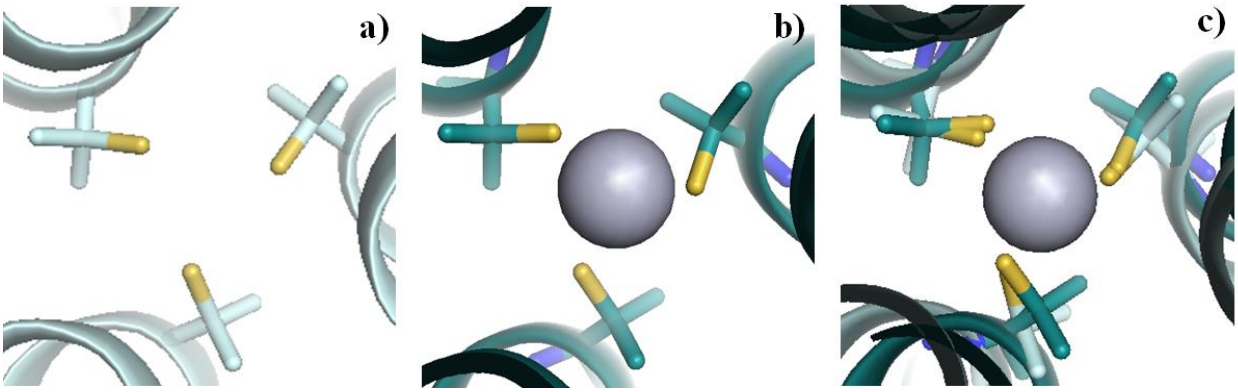

Figure S5. Structure comparison between the apo-$(CSL16Pen)_3$ (PDB code: 3H5F)[3] and $[Hg(II)]_S[Zn(II)(H_2O/OH^-)]_N(CSL9PenL23H)_3^{n+}$ (PDB code: 3PBJ)[8] demonstrating the preorganization of Pen rotamers upon Hg(II) binding in a trigonal planar geometry. Shown from the top-down view, the arrangements of Pen ligands in a) the unbound and b) metal bound forms. In c) overlay of the two structures. All the Pen rotamers in both structures point their γ-thiols to the core of the 3SCC, while the γ-methyl groups are directed to the helical interface. Main chain atoms are shown as ribbon diagrams in which the apo-structure is in pale teal and metallated-structure is in deep cyan. Pen residues are shown as sticks (sulfurs=yellow). Hg(II) in the metallated $Hg(II)]_S[Zn(II)(H_2O/OH^-)]_N(CSL9PenL23H)_3^{n+}$ is represent as a grey sphere.

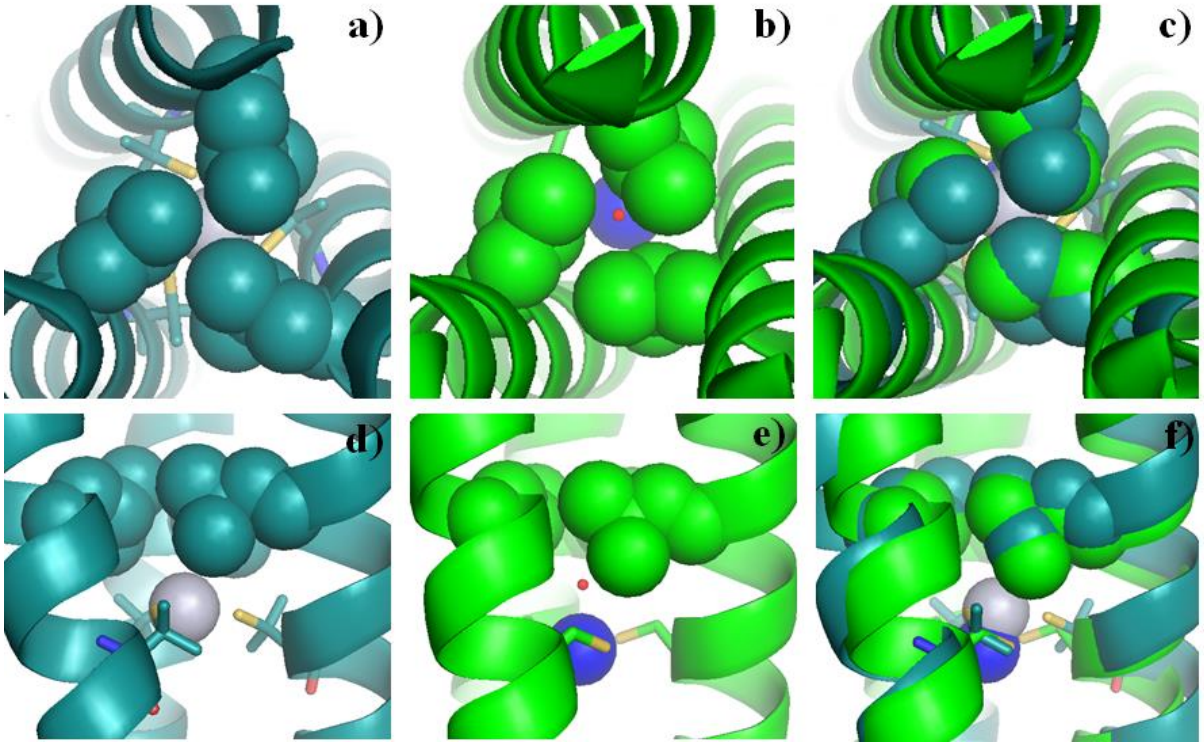

Figure S6. Packing comparison of Leu residues above the trigonal planar Hg(II) sites of $Hg(II)(S_{Cys})_3^-$ in $Hg(II)_SZn(II)_N(GRAND\text{-}CSL16CL30H)_3^+$ (PDB code: 5KB1)[7] and $Hg(II)(S_{Pen})_3^-$ in the $[Hg(II)]_S[Zn(II)(H_2O/OH^-)]_N(CSL9PenL23H)_3^{n+}$ (PDB code: 3PBJ)[8]. **Top panels**: The packing of Leu residues from the top-down view above the metal site of a) the $Hg(II)(S_{Pen})_3$ site and b) the $Hg(II)(S_{Cys})_3$ site. In c) the overlay between a) and b). Bottom panels: Side-on view of d) Leu residues above the $Hg(II)(S_{Pen})_3$, e) Leu residues above the $Hg(II)(S_{Cys})_3$ site and f) the alignment between d) and e). Main chains of $Hg(II)_SZn(II)_N(GRAND\text{-}CSL16CL30H)_3^+$ are colored in green and $[Hg(II)]_S[Zn(II)(H_2O/OH^-)]_N(CSL9PenL23H)_3^{n+}$ in cyan. Cys and Pen side chains are shown as sticks where sulfurs are yellow. Hg(II) atoms in the $[Hg(II)]_S[Zn(II)(H_2O/OH^-)]_N(CSL9PenL23H)_3^{n+}$ and $Hg(II)_SZn(II)_N(GRAND\text{-}CSL16CL30H)_3^+$ and are present as grey and blue spheres, respectively. Water is shown as small red sphere.

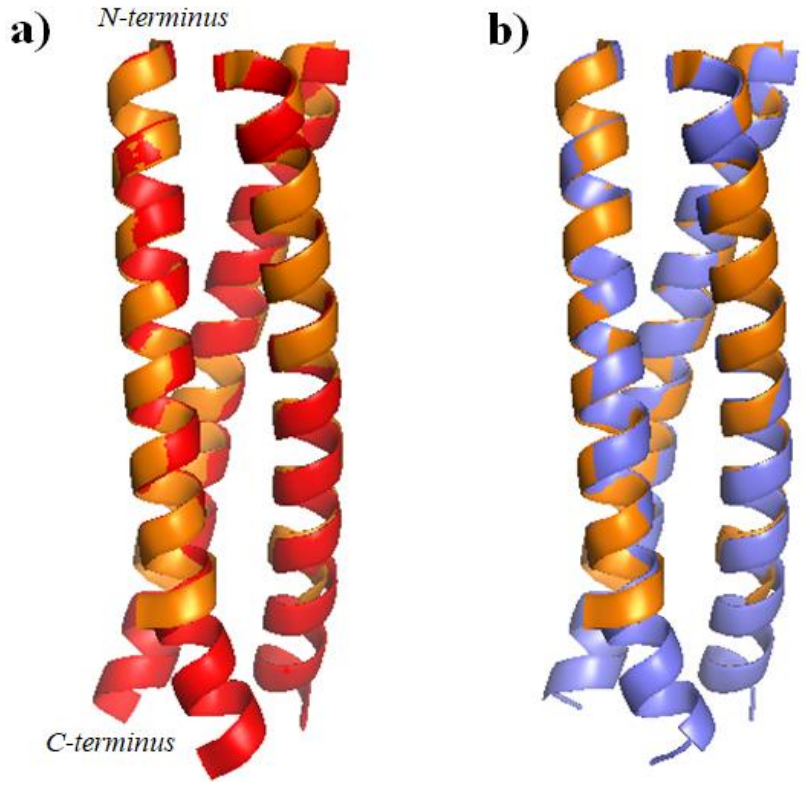

Figure S7. The backbone alignments of D-Leu containing peptide in comparison with the apo-$(CSL16C)_3$ (PDB code: 5K92)[7] demonstrating no change in the overall secondary structures when D-Leu is incorporated in the sequence. a) A comparison between apo-$(GRAND\text{-}CSL12_DLL16C)_3$ (red) and apo-$(CSL16C)_3$ (orange) (RMSD = 0.36). b) A comparison between apo-$(GRAND\text{-}CSL16CL19_DL)_3$ (blue) and apo-$(CSL16C)_3$ (orange) (RMSD = 0.41).

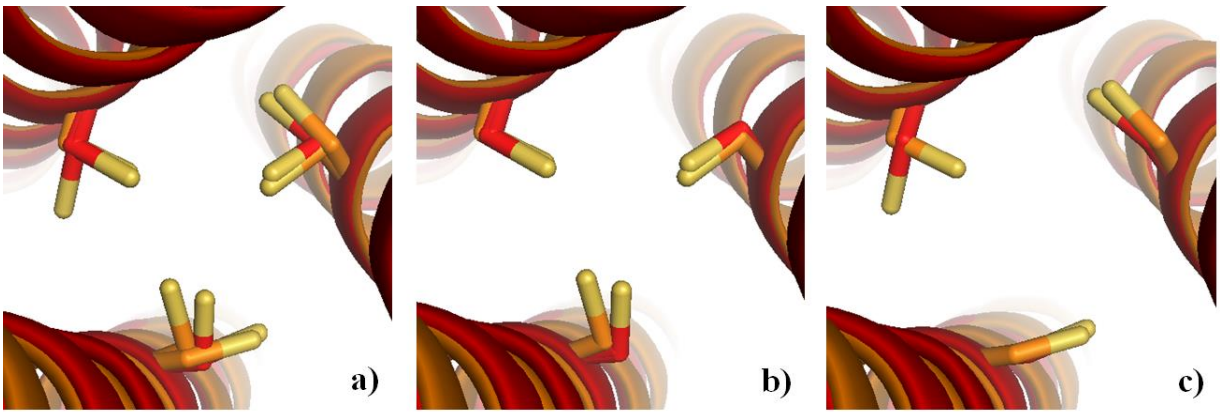

Figure S8. Overlay of the apo-(GRAND-CSL12$_D$LL16C)$_3$ and apo-(CSL16C)$_3$ (PDB code: 5K92) structures showing the orientations of Cys side chains. Top-down view from the N-termini, representing a) all Cys conformers of the two structures, b) the major conformers and c) the minor conformers. (note: In apo-(CSL16C)$_3$, only two chains contain minor conformations.) Main chain atoms are shown in red for apo-(GRAND-CSL12$_D$LL16C)$_3$ and in orange for apo-(CSL16C)$_3$. The Cys side chains are shown as sticks (sulfurs=yellow).

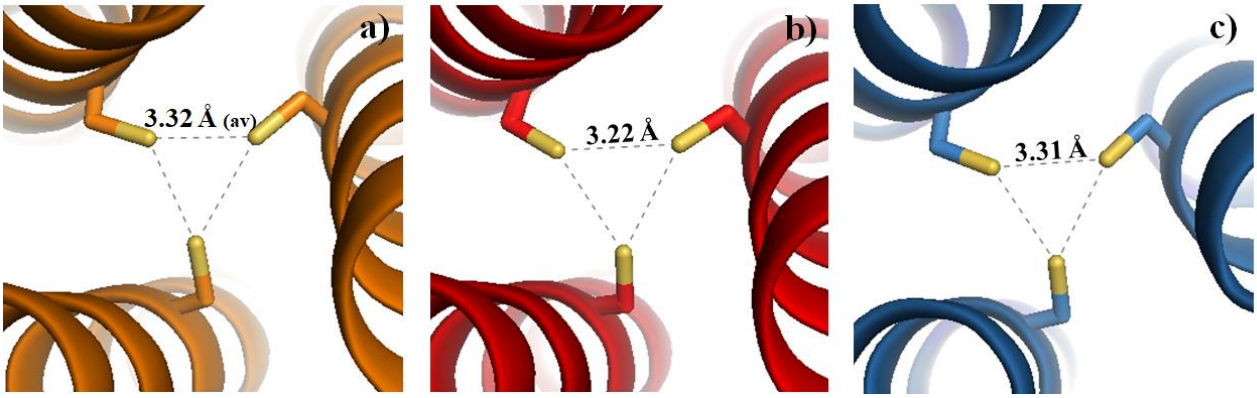

Figure S9. Ribbon diagrams shown from the top-down view of 3SCC demonstrating similarity of the Cys orientations in a) apo-$(CSL16C)_3$ (major conformer) , b) apo-$(GRAND\text{-}CSL12_DLL16C)_3$ (major conformer) and c) apo-$(GRAND\text{-}CSL16CL19_DL)_3$ structures. The Cys side chains are shown as sticks (sulfurs=yellow).

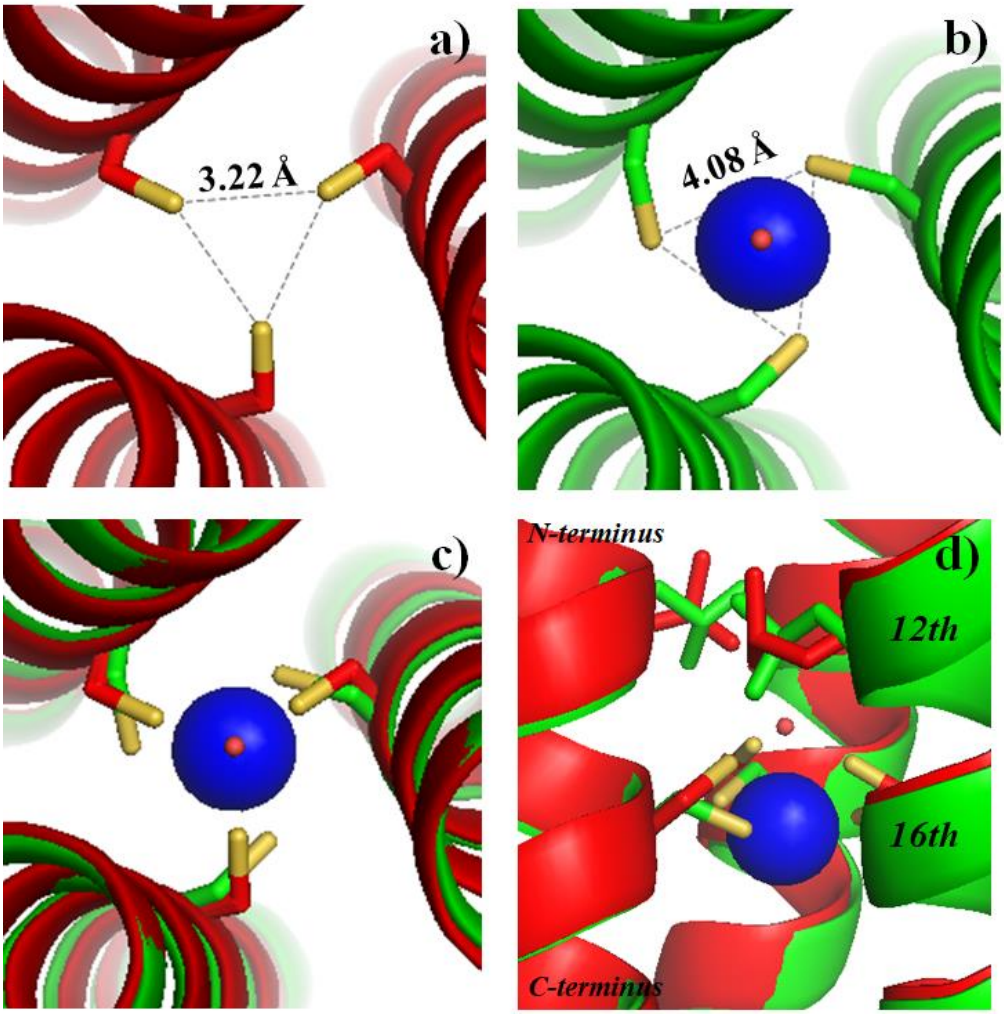

Figure S10. Ribbon diagrams demonstrating the *predisposition* of three Cys ligands of apo-(GRAND-CSL12$_D$LL16C)$_3$ toward Hg(II) binding. Top down view of the major conformer of a) unbound Cys rotamers in apo-(GRAND-CSL12$_D$LL16C)$_3$ and b) bound Cys rotamers in Hg(II)$_S$Zn(II)$_N$(GRAND-CSL16CL30H)$_3^+$ (PDB code: 5KB1)[7]. c) Top-down and d) side-on views of the overlay suggesting the rearrangement of Cys ligands required to bind Hg(II) in a trigonal planar structure. Main chain atoms of apo-(GRAND-CSL12$_D$LL16C)$_3$ are colored in red and Hg(II)$_S$Zn(II)$_N$(GRAND-CSL16CL30H)$_3^+$ in green. 16Cys, 12L-Leu and 12D-Leu side chains are shown as sticks (sulfurs=yellow). Hg(II) is present as a blue sphere and the water observed in between the 12L-Leu and 16Cys cavity is red.

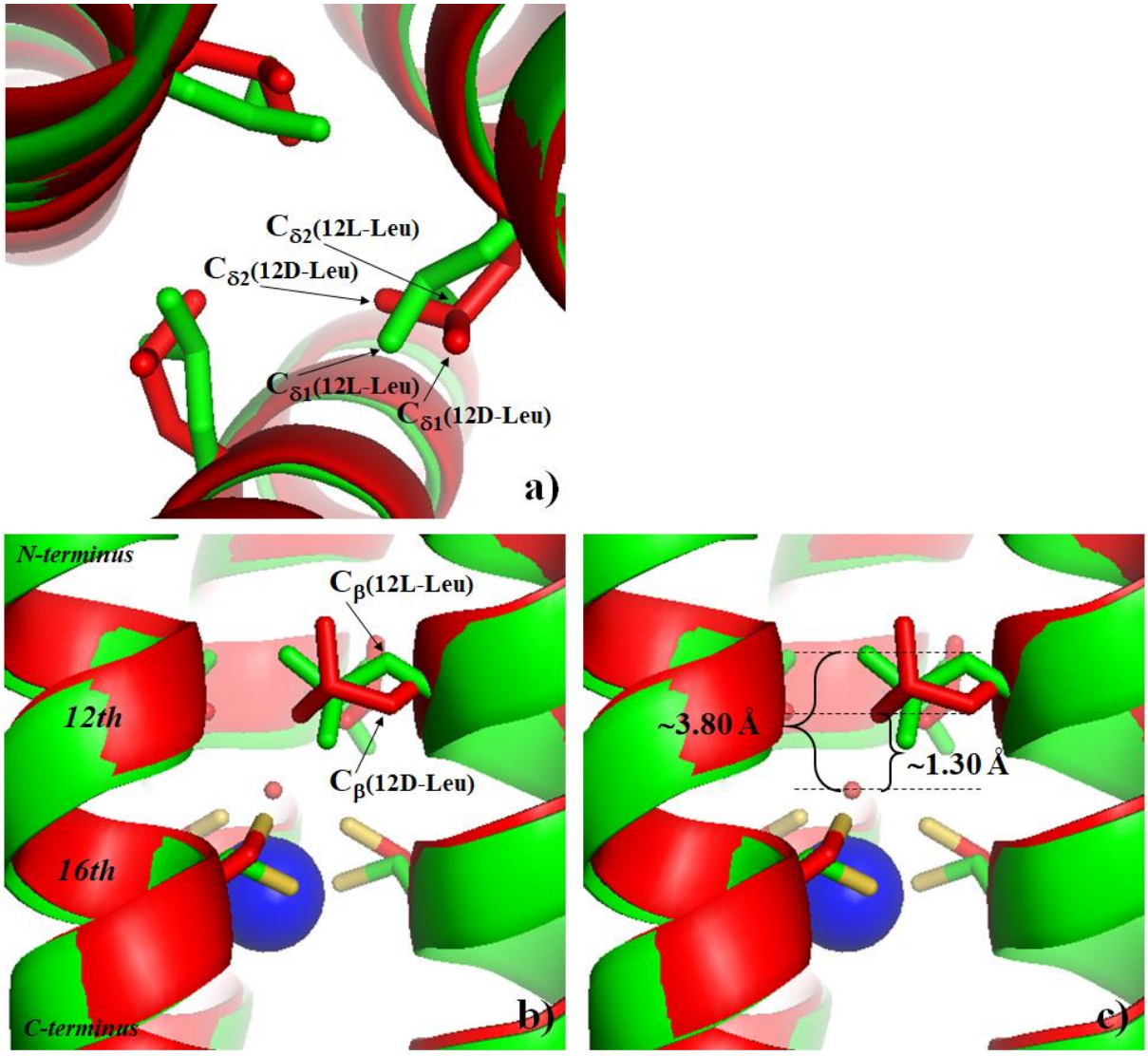

Figure S11. Overlay of apo-(GRAND-CSL12$_D$LL16C)$_3$ and Hg(II)$_S$Zn(II)$_N$(GRAND-CSL16CL30H)$_3^+$ (PDB code: 5KB1)[7]. In a) top-down and b) side-on view of the overlay representing the difference in positions of C_β, $C_{\delta1}$ and $C_{\delta2}$ atoms between 12D-Leu (red) in the apo-(GRAND-CSL12$_D$LL16C)$_3$ and 12L-Leu (green) in Hg(II)$_S$Zn(II)$_N$(GRAND-CSL16CL30H)$_3^+$. In c) distances determined from the plane generated by the core δ-methyl atom ($C_{\delta1}$) of the 12L-Leu residue to the water in Hg(II)$_S$Zn(II)$_N$(GRAND-CSL16CL30H)$_3^+$ (~3.80 Å) compared to the related distance (~1.30 Å) determined from the plane generated by the core δ-methyl atom ($C_{\delta2}$) of the 12D-Leu residue in apo-(GRAND-CSL12$_D$LL16C)$_3$ to the water in Hg(II)$_S$Zn(II)$_N$(GRAND-CSL16CL30H)$_3^+$. Main chain atoms of apo-(GRAND-CSL12$_D$LL16C)$_3$ are colored in red and Hg(II)$_S$Zn(II)$_N$(GRAND-CSL16CL30H)$_3^+$ in green. Hg(II) atom and the observed water in Hg(II)$_S$Zn(II)$_N$(GRAND-CSL16CL30H)$_3^+$ are present in blue and red spheres, respectively.

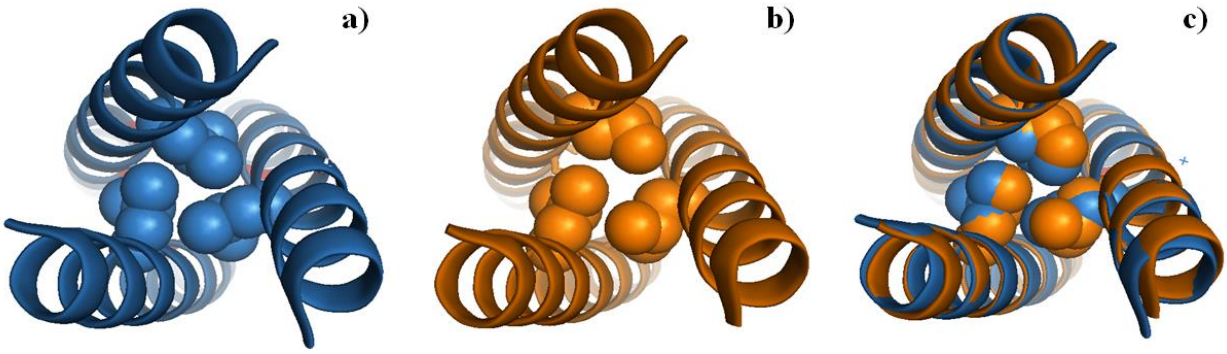

Figure S12. Packing of L-Leu residues in the twelfth position of apo-(GRAND-CSL16CL19$_D$L)$_3$ compared to apo-(CSL16C)$_3$ (PDB code: 5K92)[7]. From top down view of the N-termini, showing the packing above the metal site of a) 12L-Leu (blue) in apo-(GRAND-CSL16CL19$_D$L)$_3$, b) 12L-Leu (orange) in apo-(CSL16C)$_3$ and c) an overlay between a) and b).

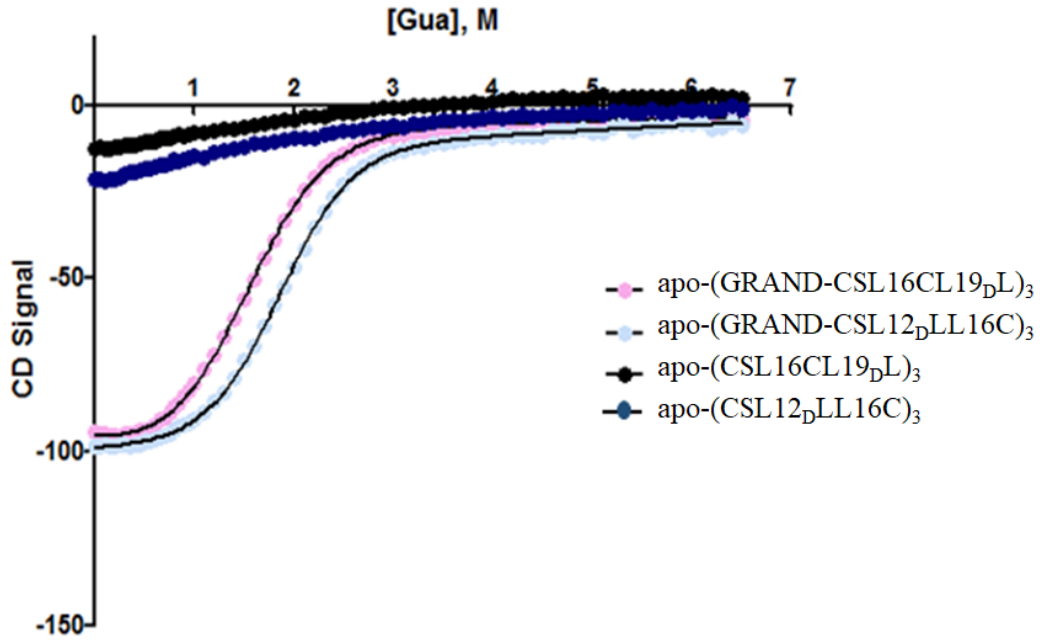

Figure S13. GuaHCl denaturation curves showing the effect of D-Leu on the GRAND-CS and CS peptides. The titrations were performed at pH 8.5, ambient temperature.

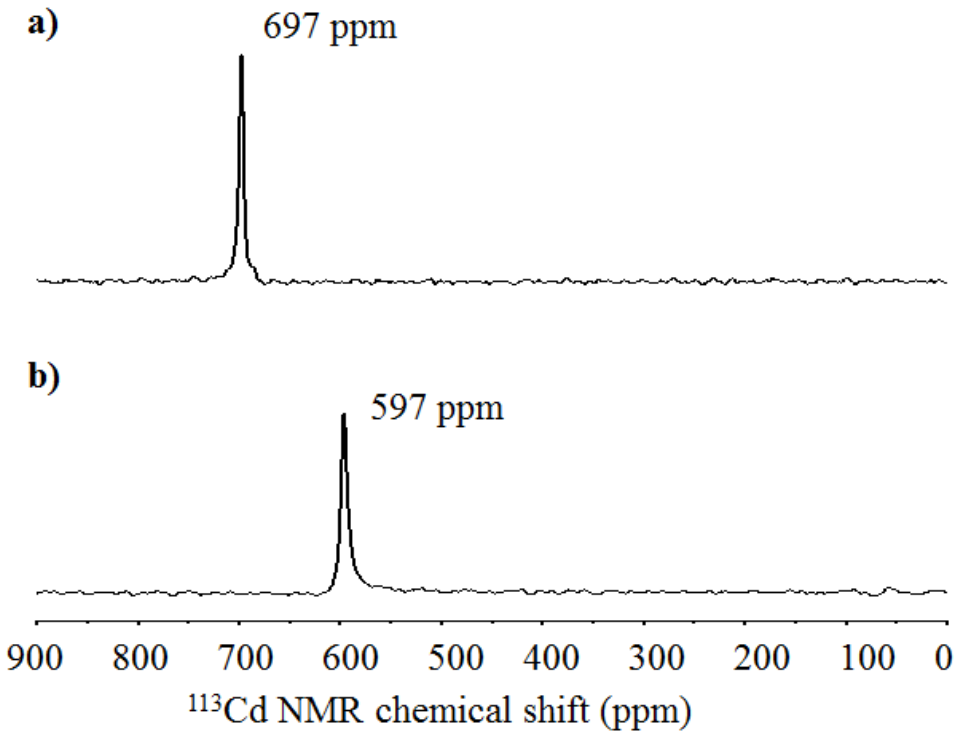

Figure S14. ^{113}Cd NMR of Cd(II)(GRAND-CSL12$_D$LL16C)$_3^-$ and Cd(II)(GRAND-CSL16CL19$_D$L)$_3^-$. The spectrum was recorded at pH 8.5.

References

(1) Chakraborty, S.; Touw, D. S.; Peacock, A. F. A.; Stuckey, J.; Pecoraro, V. L. *J. Am. Chem. Soc.* **2010**, *132* (38), 13240.

(2) Touw, D. S.; Nordman, C. E.; Stuckey, J. A.; Pecoraro, V. L. *Proc. Natl. Acad. Sci. U. S. A.* **2007**, *104* (29), 11969.

(3) Peacock, A. F. A.; Stuckey, J. A.; Pecoraro, V. L. *Angew. Chem. Int. Ed. Engl.* **2009**, *48* (40), 7371.

(4) Zastrow, M.; Pecoraro, V. L. *Coord. Chem. Rev.* **2013**, *257*, 2565.

(5) Peacock, A. F. A.; Hemmingsen, L.; Pecoraro, V. L. *Proc. Natl. Acad. Sci. U. S. A.* **2008**, *105* (43), 16566.

(6) Ruckthong, L.; Deb, A.; Hemmingsen, L.; Penner-Hahn, J. E.; Pecoraro, V. L. *J. Biol. Inorg. Chem.* **2018**, *23* (1), 123.

(7) Ruckthong, L.; Zastrow, M. L.; Stuckey, J. A.; Pecoraro, V. L. *J. Am. Chem. Soc.* **2016**, *138* (36), 11979.

(8) Zastrow, M. L.; Peacock, A. F. A.; Stuckey, J. A.; Pecoraro, V. L. *Nat. Chem.* **2012**, *4*, 118.